J Membrane Biol (2008) 221:133–140
DOI 10.1007/s00232-007-9091-3

Functional Consequences of Various Leucine Mutations in the M3/M4 Loop of the Na^+,K^+-ATPase α-Subunit

Hiroshi Eguchi · Magotoshi Morii · Yuji Takahashi · Hideki Sakai · Masahiro Nakano · Hideo Ochiai · Akira Shirahata · Yukichi Hara · Masaru Kawamura · Kazuo Takeda

Received: 17 October 2007 / Accepted: 17 December 2007 / Published online: 23 January 2008

Abstract Leucines were mutated within the sequence L^{311}ILGYTWLE^{319} of the extracellular loop flanking the third (M3) and fourth (M4) transmembrane segments (M3/M4 loop) of the *Torpedo* Na^+,K^+-ATPase α-subunit. Replacement of Leu^{311} with Glu resulted in a considerable loss of Na^+,K^+-ATPase activity. Replacement of Leu^{313} with Glu shifted the equilibrium of E_1P and E_2P toward E_1P and reduced the rate of the E_1P to E_2P transition. The reduction of the transition rate and stronger inhibition of Na^+,K^+-ATPase activity by Na^+ at higher concentrations together suggest that there is interference of Na^+ release on the extracellular side in the Leu^{313} mutant. Thus, Leu^{313} could be in the pathway of Na^+ exit. Replacement of Leu^{318} with Glu yielded an enzyme with significantly reduced apparent affinity for both vanadate and K^+, with an equilibrium shifted toward E_2P and no alteration in the transition rate. The reduced vanadate affinity is due to the lower rate of production of vanadate-reactive $[K^+_2]E_2$ caused by inhibition of dephosphorylation through reduction of the K^+ affinity of E_2P. Thus, Leu^{318} may be a critical position in guiding external K^+ to its binding site.

Keywords Access path · Extracellular loop · Leucine · K^+ · Na^+ · Na^+,K^+-ATPase

H. Eguchi · H. Ochiai · M. Kawamura (✉) · K. Takeda
Department of Cell Biology, School of Medicine, University of Occupational and Environmental Health, Kitakyushu 807-8555, Japan
e-mail: xenopus@med.uoeh-u.ac.jp

H. Eguchi · A. Shirahata
Department of Pediatrics, School of Medicine, University of Occupational and Environmental Health, Kitakyushu 807-8555, Japan

M. Morii · Y. Takahashi · H. Sakai
Department of Pharmaceutical Physiology, Graduate School of Medicine and Pharmaceutical Sciences, University of Toyama, Toyama 930-0194, Japan

M. Nakano
Department of Health Information Science, School of Health Science, University of Occupational and Environmental Health, Kitakyushu 807-8555, Japan

Y. Hara
Departments of Biochemistry and Biophysics, Tokyo Medical and Dental University, Tokyo 113-8519, Japan

Introduction

The Na^+,K^+-ATPase in the plasma membrane of animal cells transports Na^+ out of the cell and K^+ into the cell at a stoichiometry of 3:2, using the energy derived from hydrolysis of ATP (for review, see Jorgensen et al., 2003). The transport mechanism of Na^+,K^+-ATPase is based on a cyclic scheme involving two main conformations, E_1 and E_2, which link ion movement to ATP hydrolysis (Albers, 1967; Post et al., 1969). Binding of three Na^+ ions to the intracellular interface of the enzyme in the E_1 form triggers the formation of an ADP-sensitive phosphoenzyme, E_1P. E_1P spontaneously transforms into the ADP-insensitive E_2P phosphoenzyme, a process coupled to release of Na^+ on the extracellular side of the membrane. Dephosphorylation of E_2P is activated by binding of extracellular K^+, leading to formation of the E_2 conformation. Access of cations to their binding site is controlled by two gates, one on the intracellular side and one on the extracellular side (Apell & Karlish, 2001). The internal gate opens in the E_1 form to allow access of Na^+ to the intracellular side, and the external gate opens in the E_2 form to allow access of K^+

to the extracellular side. The structural basis of the gates, the gating mechanism and the access pathways to the cation binding sites are not yet fully understood.

The sarcoplasmic reticulum Ca^{2+}-ATPase has a structure similar to that of the α-subunit of Na^+,K^+-ATPase that has been determined at atomic resolution (Toyoshima et al., 2000; Toyoshima & Mizutani, 2004). The Ca^{2+}-ATPase structure has an M3/M4 loop constituting the luminal (external) gate (Toyoshima et al., 2004; Capendeguy et al., 2006). The M3/M4 loop is able to interact closely with the M7/M8 loop and thereby covers a part of the cation channel of the α-subunit of Na^+,K^+-ATPase (Yudowski et al., 2003). Based on these observations, we previously examined the effect of mutating Leu^{318} in the M3/M4 loop on the K^+ affinity of Na^+,K^+-ATPase activity (Eguchi et al., 2005). We suggested that Leu^{318} occupies a critical position in the access pathway of external K^+ ions to their binding site.

In this study, we replaced three leucine residues in the M3/M4 loop and reveal that leucine residues in this loop (Leu^{311}, Leu^{313} and Leu^{318}) play important yet varied roles in cation transport of Na^+,K^+-ATPase.

Materials and Methods

Mutagenesis and Expression

For the replacement of amino acid residues, base substitutions were introduced into the cDNA encoding the ouabain-resistant α-subunit of *Torpedo californica* Na^+,K^+-ATPase cloned into the SP65 (Noguchi et al., 1987) vector using the Quick Change mutagenesis kit (Stratagene, La Jolla, CA). All resulting cDNA sequences were verified.

Torpedo α-subunits, both wild type and mutants, were expressed with the ß-subunit in *Xenopus* oocytes by injection of the corresponding cRNAs (8.5 and 5.0 ng/oocyte for the α- and ß-subunits, respectively). Oocytes were incubated at 19°C for 60 h in modified Barth's medium (Gurdon, 1974).

Expression of wild-type and mutant α-subunits was examined by Western blot. Microsomes (containing 10 μg of protein) were resolved by electrophoresis on 10% polyacrylamide gels containing 0.1% sodium dodecyl sulfate (SDS). Separated proteins were transferred to polyvinylidene difluoride membranes. The α-subunits were detected by anti-*Torpedo* Na^+, K^+-ATPase α-subunit antisera (Noguchi et al., 1990) followed by a secondary horseradish peroxidase–conjugated anti-rabbit immunoglobulin G (Santa Cruz Biotechnology, Santa Cruz, CA) and subsequently quantified by a chemiluminescence assay (Roche Molecular Biochemicals, Mannheim, Germany).

Na^+,K^+-ATPase Activity

About 80 oocytes were homogenized, and microsomal fractions were recovered from homogenates by centrifugation at 213,000 × *g* for 20 min. Microsomes were further treated with 1 M NaSCN at 20°C for 60 min to reduce nonspecific ATPase activity. Na^+,K^+-ATPase activity was assayed at 37°C in a reaction mixture (19 μl) containing 50 mM Tris/HCl buffer (pH 7.4), 140 mM NaCl, 14 mM KCl, 5 mM $MgCl_2$, 1 mM ethyleneglycoltetraacetic acid (EGTA), 1 mM ATP, and microsomes (about 5 μg of protein) with 10 μM or 10 mM ouabain. Released inorganic phosphate was determined by the malachite green method (Lanzetta et al., 1979). Both wild-type and mutant Na^+,K^+-ATPase was ouabain-resistant and fully active in the presence of 10 μM ouabain, whereas oocyte endogenous Na^+,K^+-ATPase was nearly completely inhibited with 10 μM ouabain. Therefore, Na^+,K^+-ATPase activity associated with enzymes exogenously expressed was calculated by subtraction of ATPase activity measured at 10 mM ouabain, where all of the Na^+,K^+-ATPase was inhibited, from that measured at 10 μM ouabain. The activities thus obtained were divided by the respective amounts of α-subunit quantified by Western blot analysis, yielding apparent specific activities. The apparent specific activities were normalized to the wild-type activity, and the resulting activity of each mutant obtained from each experiment was averaged.

Phosphoenzyme Studies

ADP-dependent dephosphorylation was assayed as follows (Jensen & Vilsen, 2002). Microsomes from cRNA-injected oocytes were phosphorylated for 15 s at 0°C in the presence of 10 mM NaCl, 20 mM Tris/HCl (pH 7.4), 3 mM $MgCl_2$, 1 mM EGTA, 10 μM ouabain and 2 μM [γ-^{32}P]ATP. Dephosphorylation was initiated by adding a chase solution yielding final concentrations of 2.5 mM ADP and 1 mM unlabeled ATP, followed by acid quenching. Dephosphorylation in the presence of K^+ ($E_1P \rightarrow E_2P$ transition) was assayed by using phosphoenzyme formed at 600 mM NaCl (to accumulate E_1P), 20 mM Tris/HCl (pH 7.4), 3 mM $MgCl_2$, 1 mM EGTA, 10 μM ouabain and 2 μM [γ-^{32}P]ATP at 0°C for 15 s (Klodos et al., 1994). Dephosphorylation was initiated by adding a chase solution yielding final concentrations of 600 mM NaCl, 20 mM KCl and 1 mM unlabeled ATP, followed by acid quenching. The acid-quenched precipitates were washed by centrifugation and acidic SDS-polyacrylamide gel electrophoresis was performed (Sarkadi et al., 1986). The narrow 95-kDa protein band associated with radioactivity was quantified by FLA5000 (Fujix, Tokyo, Japan).

Homology Modeling of the *Torpedo* Na^+,K^+-ATPase α-Subunit

Amino acid sequences of the transmembrane helices and extracellular loops of *Torpedo* Na^+,K^+-ATPase α-subunits (P05025) were aligned with those of the rabbit sarcoplasmic reticulum Ca^{2+}-pump (P04191-2) using the gapped BLAST program (Thompson et al., 1994) with default parameters. Then, multiple alignments were obtained by the CLUSTALW program (Ogawa & Toyoshima, 2002) to reduce the possibility of different alignments, under the assumption that lipid-facing residues tend to be variable whereas those involved in helix–helix contacts tend to be conserved (Thompson et al., 1994; Ogawa & Toyoshima, 2002). Aligned sequences were inspected and adjusted manually to avoid gaps within the transmembrane helices. The three-dimensional (3-D) structure models of *Torpedo* Na^+,K^+-ATPase α-subunit were constructed using the MODELLER program (Sali & Blundell, 1993) based on the atomic models of the E_1P (1wpe.pdb) and E_2P (1wpg.pdb) of rabbit sarcoplasmic reticulum Ca^{2+}-ATPase with restriction of partial structures. Structures of long insertion (Met^1–Val^{39} and His^{665}–Thr^{685}) were restricted to the predicted structures obtained by PredictProtein (Rost et al., 2004). To obtain stable structures after homology modeling, energy minimization at constant temperature 300 K was carried out using the AMBER 8 program (Pearlman et al., 1995) after addition of 23 neutralizing Na^+ ions. Calculations were performed using a Linux high-performance cluster computer system (32 CPUs). Models were visualized by the VMD program (Humphrey et al., 1996) and the DS ViewerPro 5.0 program (Accelrys Software, San Diego, CA).

Data Analysis

The Na^+ and K^+ dependence of ATPase activity and phosphoenzyme studies were analyzed by a nonlinear curve fitting program using Prism 3.0 (GraphPad Software, San Diego, CA), and the best fits are shown as lines in the figures. The Na^+ and K^+ concentration dependences were fitted to the Hill equation. The phosphoenzyme decay curves were obtained by fitting the data points to the sum of two exponentials:

$$\% \text{ phosphorylation} = (100\% - a)e^{-k_1 t} + ae^{-k_2 t}$$

where k_1 and k_2 represent the rate coefficients of the rapid and slow components, respectively, of the decay curve and a is the extent of the slow component (Vilsen, 1997).

Results

Protein Expression

The relative expression levels of wild-type and mutant Na^+,K^+-ATPase were examined by Western blot analysis. As shown in Figure 1, the expression levels of the α-subunits varied from mutant to mutant but each of the mutants expressed sufficient quantities, which enabled examination of their functional characteristics. The Na^+,K^+-ATPase activity of the mutants was corrected according to the level of expression as described in "Materials and Methods."

Glutamic Acid Mutants of the M3/M4 Loop

The α-subunit of *Torpedo* Na^+,K^+-ATPase contains a single glutamic acid (Glu^{319}) in the nine–amino acid M3/M4 extracellular short loop ($L^{311}ILGYTWLE^{319}$). In the previous study, we replaced three residues of this loop, one residue at a time from Thr^{316} to Leu^{318}, with glutamic acid in the construct with Glu^{319} already mutated to Gln (E scanning) and showed that mutation of Leu^{318} resulted in lower apparent K^+ affinity for ATPase activity (Eguchi et al., 2005). Here, we continued E scanning toward the N-terminal side of this loop, excluding Tyr^{315} which is involved in ouabain binding (Canessa et al., 1993), and examined the Na^+,K^+-ATPase activity of the resulting mutants. The results are shown in Figure 2A together with the activities of the C-terminal mutants reported previously. With the exception of the L311E/E319Q and L313E/E319Q mutants, all mutants showed significant Na^+,K^+-ATPase activity, ranging from 45 ± 5% (average of three

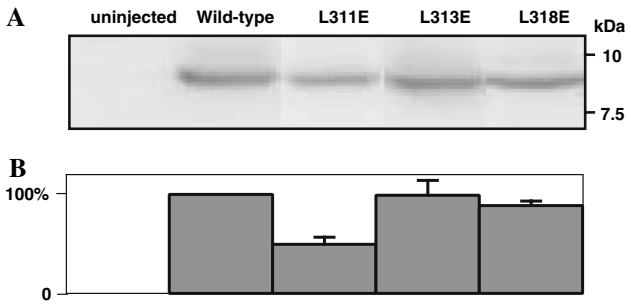

Fig. 1 Expression of mutants. (**A**) Microsomes (10 μg of total protein/lane) isolated from oocytes injected with cRNA for the α-subunit (cRNAs are indicated above the respective lanes) together with cRNA for the β-subunit were subjected to Western analysis and incubated with a polyclonal anti-*Torpedo* Na^+,K^+-ATPase α-subunit antibody. (**B**) Quantified data for the respective lanes are provided below the blot

independent experiments) for G314E/E319Q to 106 ± 10% (average of four independent experiments) for T316E/E319Q relative to the activity of the wild type. The activities of L311E/E319Q and L313E/E319Q were 7% and 4% (averages of two independent experiments), respectively, suggesting that Leu^{311} and Leu^{313}, solely or in combination with Glu^{319}, play important roles in ATPase activity. In order to examine whether the lower activity of these two mutants was due to the simultaneous mutations of Leu^{311} or Leu^{313} and Glu^{319} in the M3/M4 loop or the possible indispensability of Leu^{311} and Leu^{313} in ATPase activity, we replaced Leu^{311} and Leu^{313} with Glu, Asp, Gln and Asn in the wild type α-subunit cDNA (single mutant). The results are shown in Figure 2B. The ATPase activity of Leu^{311} single mutants ranged between 30% and 40% of the wild type, while those of Leu^{313} mutants were substantially recovered with activities from 60% to 110%. In this report, we focused on single mutants of Leu^{311} and Leu^{313} replaced with Glu together with Leu^{318}, which has been previously revealed to be involved in the access path of K^+ (Eguchi et al., 2005). All these leucines are well conserved in Na^+,K^+-ATPase.

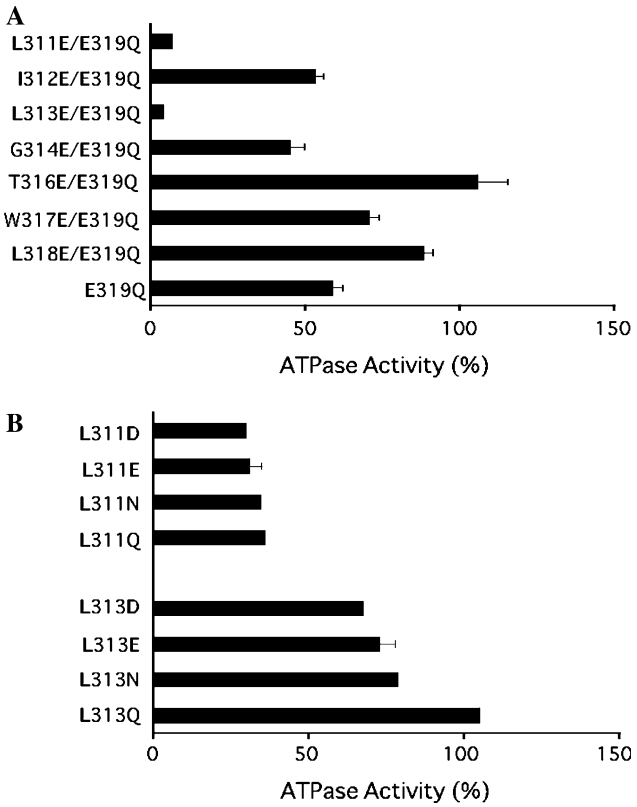

Fig. 2 Na^+,K^+-ATPase activity of mutants. ATPase activity of glutamic acid mutants of the M3/M4 loop with Glu^{319} already mutated to Gln (**A**) and of Leu^{311} and Leu^{313} mutants constructed from wild type α-subunit (**B**). The activities are presented relative to the wild type. Activities without error bars are averages of two independent experiments

Na^+ and K^+ Dependence of Na^+,K^+-ATPase Activity

Titration of the Na^+ dependence of ATPase activity showed little difference, if any, in the L311E, L313E and L318E mutants in the apparent affinity for Na^+ (Fig. 3A, Table 1). However, as shown in Figure 3A (inset), L313E was rather strongly inhibited by higher Na^+ concentrations in comparison with L311E, L318E and wild type. The apparent affinity for K^+ of L311E and L313E was nearly the same as that of wild type, while that of L318E was significantly reduced, as reported previously (Eguchi et al., 2005) (Fig. 3B, Table 1).

Vanadate Sensitivity of Na^+,K^+-ATPase Activity

Vanadate inhibits Na^+,K^+-ATPase by binding preferentially to the $[K^+_2]E_2$ form of the enzyme (Cantley et al., 1978). Figure 4 shows titration of the vanadate inhibition of Na^+,K^+-ATPase activity in the wild type and mutants L311, L313E and L318E. Compared with the wild type, the vanadate affinity was reduced 3.5- and 2.3-fold in L313E and L318E, respectively, while that of L311E was nearly unchanged. Ligand concentration giving half-maximum effect, $K_{0.5}$ values for vanadate for the mutants are shown in Table 1.

ADP Sensitivity of the Phosphoenzyme

Next, we analyzed the partition of the phosphoenzyme between E_1P and E_2P by studying ADP-sensitive dephosphorylation at 0°C. Figure 5 shows the time course of dephosphorylation initiated by addition of 2.5 mM ADP together with 1 mM unlabeled ATP to phosphoenzyme formed from $[\gamma^{32\text{-}P}]$ATP. Phosphorylation as well as dephosphorylation were performed in the presence of 10 mM Na^+ and the absence of K^+. Under these conditions, E_1P_1 dephosphorylates rapidly because of its ability to donate a phosphoryl group back to ADP, thus forming ATP, whereas ADP-insensitive E_2P dephosphorylates very slowly. Thus, the data points representing the time course of dephosphorylation could be fitted by a biexponential function where the extents of the rapid and slow decay components reflect the initial amounts of the ADP-sensitive E_1P and ADP-insensitive E_2P, respectively. The time course curve of dephosphorylation was fitted using a biexponential function as described in "Materials and Methods," and the initial amounts of ADP-sensitive E_1P and ADP-insensitive E_2P were estimated by the extents of the rapid and slow decay components, respectively. The ratios of E_1P/E_2P thus obtained are shown in Table 1. The amount of E_1P for L311E was 45% and equal to that in the wild type. For L313E, the amount of E_1P increased to 75%, and hence the distribution of E_1P and E_2P in L313E was more in favor of E_1P than the

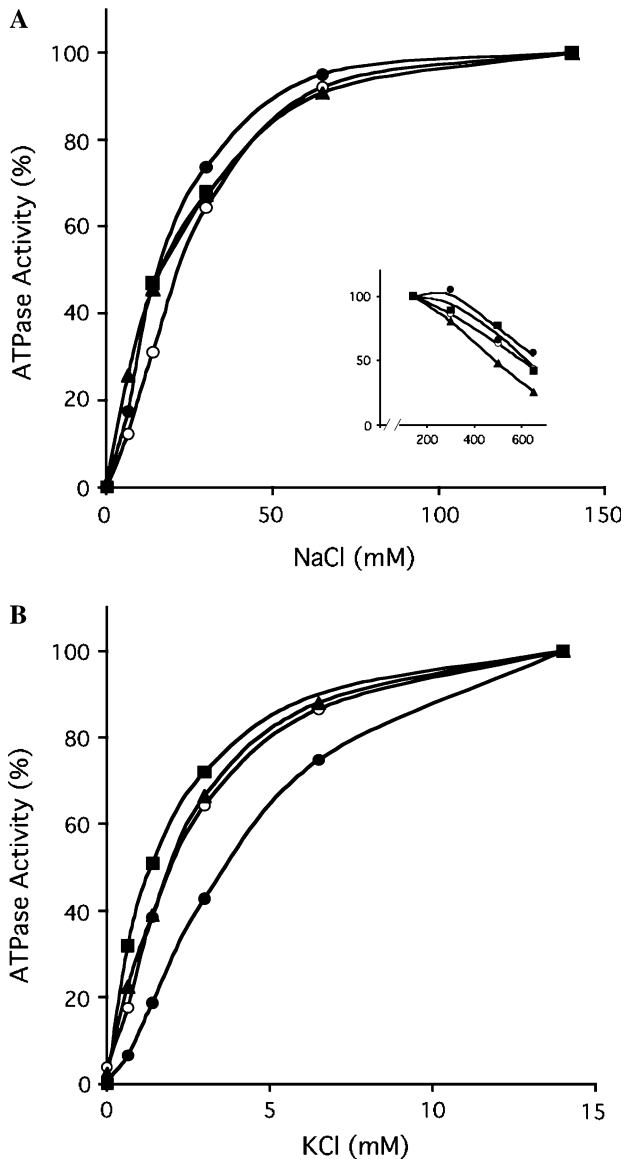

Fig. 3 Na^+ and K^+ dependence of ATPase activity. Wild type (○), L311E (■), L313E (▲) and L318E (•) were assayed as described in "Materials and Methods." Data points are the values averaged following normalization to the maximum activity at 140 mM NaCl (**A**) or 14 mM KCl (**B**). At least three independent assays were carried out corresponding to each line. For all data points, the standard error of the mean was <5%. The $K_{0.5}$ determined by fitting the Hill equation is shown in Table 1. **A** Na^+ dependence, assayed in 14 mM KCl. (*Inset*) Inhibition of ATPase activity by higher Na^+ concentrations. **B** K^+ dependence, assayed in 140 mM NaCl

wild type. In contrast, E_1P of the L318E mutant was 25% of the phosphoenzyme, lower than in the wild type.

Dephosphorylation of Phosphoenzyme ($E_1P \rightarrow E_2P$ Transition)

To examine whether a change in the rate of the $E_1P \rightarrow E_2P$ transition may be involved in the change of distribution of E_1P and E_2P, dephosphorylation of the phosphoenzyme at 600 mM Na^+ was assayed. This rate of dephosphorylation reflects the rate of the E_1P to E_2P transition (Klodos et al., 1994). Dephosphorylation was started by addition of a chase solution producing final concentrations of 600 mM Na^+, 1 mM unlabeled ATP and 20 mM K^+. The time courses of dephosphorylation shown in Figure 6 are nearly the same and significantly slower in L318E and L313E, respectively, compared to the wild type. The time course of dephosphorylation of L311E was similar to that of wild type. The half-lives of the phosphoenzyme in $E_1P \rightarrow E_2P$ transition are shown in Table 1. The reduced rate of $E_1P \rightarrow E_2P$ transition in L313E could cause the shift of the distribution of E_1P and E_2P in favor of E_1P.

Discussion

The reaction steps of Na^+,K^+-ATPase linking ion transport and ATP hydrolysis through conformational changes are described by the Post-Albers (E_1-E_2) scheme. Phosphorylation is triggered by binding of three intracellular Na^+ ions to the E_1 form. The translocation of Na^+ occurs in connection with a conformational change in the phosphoenzyme, $E_1P[Na^+_3] \rightarrow E_2P$ transition, which drives Na^+ to the extracellular side. The countertransport of K^+ is associated with dephosphorylation of E_2P by binding of two extracellular K^+ ions, $E_2P+2K^+ \rightarrow E_2PK^+_2 \rightarrow E_2[K^+_2]+Pi$.

The M3/M4 loop targeted in this study has a critical position at the outer mouth of the cation pathway in Na^+,K^+-ATPase, and mutations introduced in this loop might influence exit of Na^+ as well as entry of K^+.

Replacement of Leu^{318} reduced the apparent affinity for K^+ (Fig. 3; Eguchi et al., 2005) and for vanadate (Fig. 4) and shifted the equilibrium between E_1P and E_2P toward E_2P (Fig. 5) without changing the rate of the $E_1P \rightarrow E_2P$ transition (Fig. 6). Hence, replacement of Leu^{318} yielded an enzyme with a lower rate of production of vanadate-reactive E_2 ($[K^+_2]E_2$) with a higher level of E_2P, indicating that the rate of either or both of the partial reactions after E_2P ($E_2P+2K^+ \rightarrow K^+_2E_2P \rightarrow [K^+_2]E_2+Pi$) was reduced by the replacement. The reduction of the rate of the former step ($E_2P+2K^+ \rightarrow K^+_2E_2P$) must be brought about by reduction of K^+ affinity of E_2P through changes in the process of external K^+ binding. Leu^{318} at an extracellular entrance position could play a role in directing K^+ ions to their binding sites. Mutations of Leu^{318} may cause structural and electrostatic perturbations in the access path of K^+, leading to reduction in the apparent affinity for extracellular K^+.

Mutation of Leu^{313} to Glu resulted in the accumulation of E_1P (75%) and a decrease in the rate of $E_1P \rightarrow E_2P$ transition without significant alteration in the apparent cation affinity (Table 1). The accumulation of E_1P favors

Table 1 Summary of mutational effects

Mutant	ATPase activity (%)[a]	$K_{0.5}$ (mM)[b]		Vanadate sensitivity $K_{0.5}$ (μM)[c]	E_1P/E_2P (%)[d]	E1P→E2P half-life (s)[e]
		Na^+	K^+			
Wild type	100	21 ± 2	1.9 ± 0.1	3.5 ± 0.3	45/55	0.73
L311E	31 ± 4	17 ± 7	1.4 ± 0.5	2.8 ± 0.7	45/55	0.50[f]
L313E	73 ± 5	16 ± 3	1.9 ± 0.4	12.3 ± 0.7	75/25	1.70
L318E	94 ± 7	16 ± 2	3.3 ± 0.3	8.1 ± 0.6	25/75	0.72

[a] From Figure 2

[b] From Figure 3

[c] From Figure 4

[d] From Figure 5

[e] From Figure 6

[f] Average of two independent experiments

the reduction of vanadate sensitivity in L313E. The reduction in the rate of conformational change from E_1P to E_2P in this mutant is likely due to obstruction of Na^+ exit from the binding site to the extracellular side. The stronger inhibition by Na^+ of L313E at higher concentrations than of the wild type (Fig. 3A, inset) favors this hypothesis since the inhibition is due to inhibition of the process of Na^+ exit at the extracellular side by high extracellular concentration of Na^+. Leu^{313} should be involved in the pathway for Na^+ exit.

Mutation of Leu^{311} resulted in a considerable loss of ATPase activity. Since no significant changes in all the kinetic properties examined in this study were induced by the mutation, we could not claim what defects in the mutant brought about the loss of ATPase activity.

Capendeguy et al. (2006) studied the effect of mutation in the M3/M4 loop and observed an alteration in the affinity for K^+ as a consequence of mutation. They targeted Glu^{314} (Gly^{314} in *Torpedo* enzyme), Tyr^{315}, Trp^{317} and

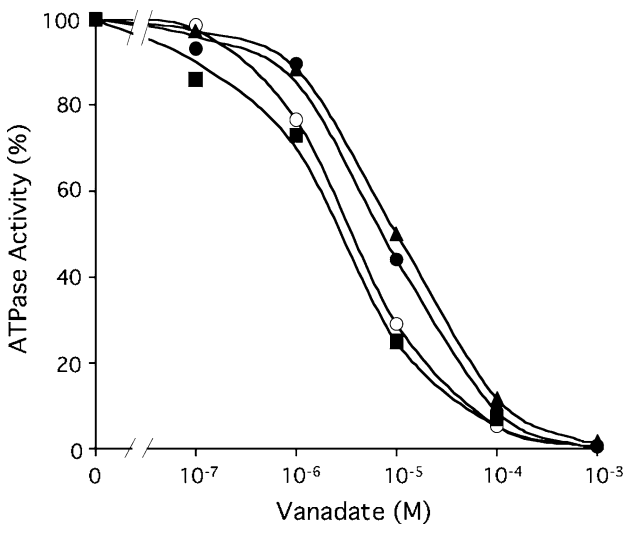

Fig. 4 Vanadate dependence of Na^+,K^+-ATPase activity. The ATPase activities of wild type (○), L311E (■), L313E (▲) and L318E (•) were assayed in the presence of 140 mM NaCl, 14 mM KCl, 1 mM ATP and the indicated concentrations of vanadate. Averaged values corresponding to three to nine independent titrations are shown as a percentage of the Na^+,K^+-ATPase activity measured in the absence of vanadate

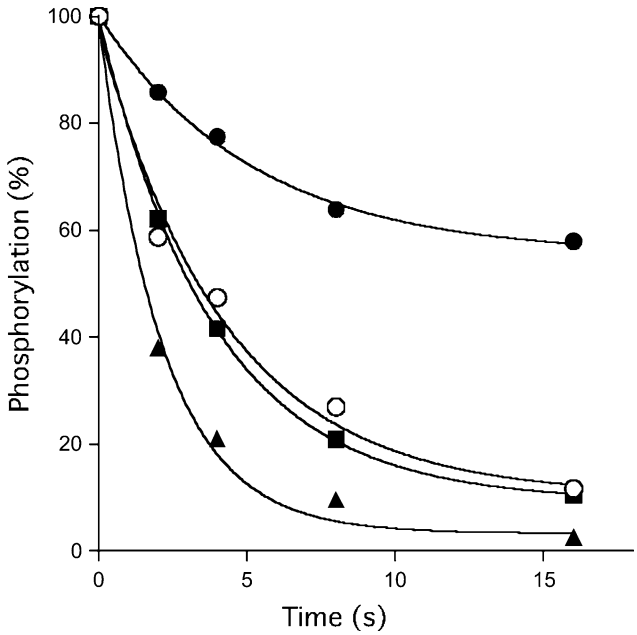

Fig. 5 Time course of ADP-dependent dephosphorylation. The wild type (○), L311E (■), L313E (▲) and L318E (•) were phosphorylated for 15 s at 0°C in the presence of 10 mM NaCl, 20 mM Tris/HCl (pH 7.4), 3 mM $MgCl_2$, 1 mM EGTA, 10 μM ouabain and 2 μM [γ-^{32}P]ATP. Dephosphorylation was started by addition of a chase solution yielding final concentrations of 2.5 mM ADP and 1 mM unlabeled ATP, followed by acid quenching at the indicated time intervals. Data points are average values of three independent experiments and are shown as a percentage of the phosphorylation level obtained after 15 s phosphorylation without the chase solution. Each line shows the best fit of a biexponential time function (see "Materials and Methods") giving the E_1P/E_2P ratio shown in Table 1

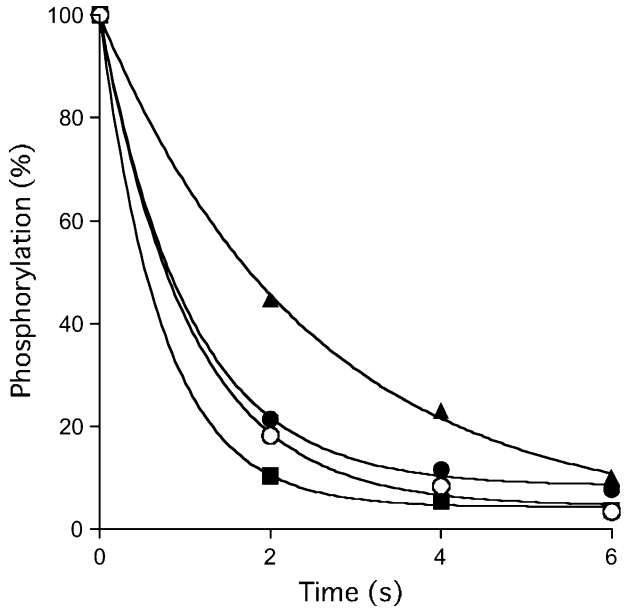

Fig. 6 Time course of dephosphorylation of phosphoenzyme in the presence of K^+. The wild type (○), L311E (■), L313E (▲) and L318E (•) were phosphorylated for 15 s at 0°C in the presence of 600 mM NaCl, 20 mM Tris/HCl (pH 7.4), 3 mM $MgCl_2$, 1 mM EGTA, 10 μM ouabain and 2 μM [γ-^{32}P]ATP. Dephosphorylation was started by addition of a chase solution yielding a final concentration of 600 mM NaCl, 20 mM KCl and 1 mM unlabeled ATP, followed by acid quenching at the indicated time intervals. The data are average values of three or four independent experiments and are shown as a percentage of phosphorylation level obtained after 15 s phosphorylation without the chase solution

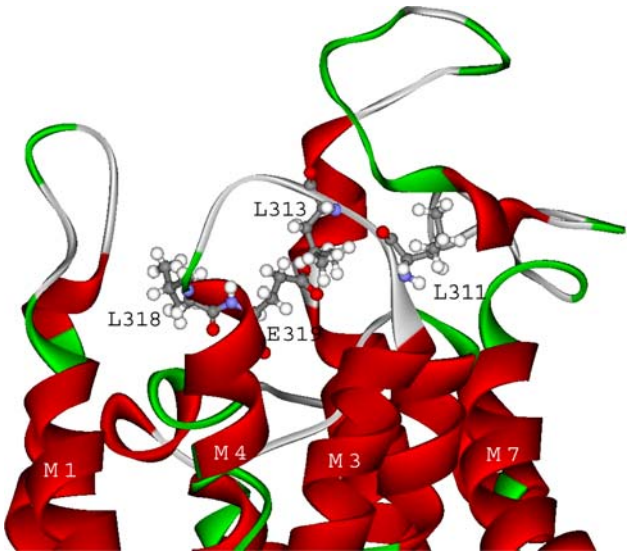

Fig. 7 Structural model of the M3/M4 loop of the Na^+,K^+-ATPase α-subunit in the E_1P state. The panel shows a view parallel to the membrane plane with the extracellular side up. The M3/M4 loop is shown with the side chains of four residues studied in this report. Carbon atoms are indicated in *gray*, oxygen atoms in *red* and nitrogen atoms in *blue*. The side chain of Leu^{318} points toward M1 and the putative cation pathway. The closeness between the side chains of Leu^{313} and Glu^{319} is seen

Ile^{322} and claimed that mutations of these residues to cysteine resulted in major increases in apparent affinity for extracellular K^+. However, the variance of apparent K^+ affinity of mutants in the M3/M4 loop that we report in a previous study (Trp^{317} and Glu^{319}) (Eguchi et al., 2005) and here (Leu^{311} and Leu^{313}) was within the range of experimental error compared to the wild type. This may be due to the difference in the site of mutation and the type of amino acid used for replacement.

Both single mutants, L313E and E319Q, were essentially active in ATPase activity (Fig. 2). When mutations were combined, however, the resulting double mutants, L313E/E319Q, lost almost all their ATPase activity. Leu^{313} should play a crucial role in the correct folding of the M3/M4 loop with the cooperation of Glu^{319}. In order to discuss possible structural effects of these mutations, a structural model of Na^+,K^+-ATPase built by homology to the structure of Ca^{2+}-ATPase would be helpful. According to the homology model of the M3/M4 loop in the E_1P conformation (Fig. 7), the side chains of Leu^{313} and Glu^{319} in the wild type are close but far from van der Waals distance. When mutated simultaneously, the mutated amino acid residues contact each other in the E_2P conformation by a hydrogen bond between the side chain amide nitrogen in Gln^{319} and the side chain carboxylate oxygen in Glu^{313} (not shown), which may be involved in loss of activity of L313E/E319Q.

In summary, Leu^{313} is in the pathway of Na^+ exiting from its binding site. Leu^{318} is at a position to guide external K^+ to its binding site. Thus, the M3/M4 loop of the Na^+,K^+-ATPase α-subunit plays an important role in external cation transport.

Acknowledgements This work was funded by a University of Occupational and Environmental Health Grant for Advanced Research to M. K.

References

Albers RW (1967) Biochemical aspects of active transport. Annu Rev Biochem 36:727–756

Apell H-J, Karlish SJD (2001) Functional properties of Na,K-ATPase, and their structural implications, as detected with biophysical techniques. J Membr Biol 180:1–9

Canessa CM, et al. (1993) Mutation of a tyrosine in the H3–H4 ectodomain of Na,K-ATPase confers ouabain resistance. J Biol Chem 268:17722–17726

Cantley LC Jr, et al. (1978) A characterization of vanadate interactions with the (Na,K)-ATPase. Mechanistic and regulatory implications. J Biol Chem 253:7361–7368

Capendeguy O, et al. (2006) Access of extracellular cations to their binding sites in Na,K-ATPase: role of the second extracellular loop of the α subunit. J Gen Physiol 127:341–352

Eguchi H, et al. (2005) Involvement in K^+ access of Leu^{318} at the extracellular domain flanking M3 and M4 of the Na^+,K^+-ATPase α-subunit. Biochem Biophys Res Commun 330:611–614

Gurdon JB (1974) The control of gene expression in animal development. Clarendon Press, Oxford

Humphrey W, et al. (1996) VMD: visual morecular dynamics. J Mol Graph 14:33–38

Jensen M, Vilsen B (2002) Importance of Glu^{282} in transmembrane segment M3 of the Na^+,K^+-ATPase for control of cation interaction and conformational changes. J Biol Chem 277:38607–38617

Jorgensen PL, et al. (2003) Structure and mechanism of Na,K-ATPase: functional sites and their interactions. Annu Rev Physiol 65:817–849

Klodos I, et al. (1994) Kinetic heterogeneity of phosphoenzyme of Na,K-ATPase modeled by unmixed lipid phases. Competence of the phosphointermediate. J Biol Chem 269:1734–1743

Lanzetta PA, et al. (1979) An improved assay for nanomole amounts of inorganic phosphate. Anal Biochem 100:95–97

Noguchi S, et al. (1987) Expression of functional $(Na^+ + K^+)$-ATPase from cloned cDNAs. FEBS Lett 225:27–32

Noguchi S, et al. (1990) A possible role of the β-subunit of (Na,K)-ATPase in facilitating correct assembly of the a-subunit into the membrane. J Biol Chem 265:15991–15995

Ogawa H, Toyoshima C (2002) Homology modeling of the cation binding sites of Na^+,K^+-ATPase. Proc Natl Acad Sci USA 99:15977–15982

Pearlman DA, et al. (1995) AMBER, a package of computer programs for applying molecular mechanics, normal mode analysis, molecular dynamics and free energy calculations to simulate the structural and energetic properties of molecules. Comp Phys Commun 91:1–41

Post RL, et al. (1969) Flexibility of an active center in sodium-plus-potassium adenosine triphosphatase. J Gen Physiol 54:306s–326s

Rost B, et al. (2004) The predictprotein server. Nucleic Acids Res 32 (Web Server issue):W321–W326

Sali A, Blundell TL (1993) Comparative protein modelling by satisfaction of spatial restraints. J Mol Biol 234:779–815

Sarkadi B, et al. (1986) Molecular characterization of the in situ red cell membrane calcium pump by limited proteolysis. J Biol Chem 261:9552–9557

Thompson JD, et al. (1994) CLUSTAL W: improving the sensitivity of progressive multiple sequence alignment through sequence weighting, position-specific gap penalties and weight matrix choice. Nucleic Acids Res 22:4673–4680

Toyoshima C, et al. (2000) Crystal structure of the calcium pump of sarcoplasmic reticulum at 2.6A resolution. Nature 405:647–655

Toyoshima C, et al. (2004) Lumenal gating mechanism revealed in calcium pump crystal structures with phosphate analogues. Nature 432:361–368

Toyoshima C, Mizutani T (2004) Crystal structure of the calcium pump with a bound ATP analogue. Nature 430:529–535

Vilsen B (1997) Leucine 332 at the boundary between the fourth transmembrane segment and the cytoplasmic domain of Na^+,K^+-ATPase plays a pivotal role in the ion translocating conformational changes. Biochemistry 36:13312–13324

Yudowski GA, et al. (2003) Evidence for tryptophan residues in the cation transport path of the Na^+,K^+-ATPase. Biochemistry 42:10212–10222